AD_____

Award Number: W81XWH-10-1-0614

TITLE:
Laser Capture Microdissection Assisted Identification of Epithelial MicroRNA Expression Signatures for Prognosis of Stage I NSCLC

PRINCIPAL INVESTIGATOR:
Sai Yendamuri, MD

CONTRACTING ORGANIZATION: Health Research, Inc.
Buffalo, NY 14263

REPORT DATE: December 2014

TYPE OF REPORT: Final

PREPARED FOR: U.S. Army Medical Research and Materiel Command
Fort Detrick, Maryland 21702-5012

REPORT DOCUMENTATION PAGE

Form Approved
OMB No. 0704-0188

1. REPORT DATE	2. REPORT TYPE	3. DATES COVERED
December 2014	Final	7Sep2010 - 30Sep2014

4. TITLE AND SUBTITLE
Laser Capture Microdissection Assisted Identification of Epithelial MicroRNA Expression Signatures for Prognosis of Stage I NSCLC

5a. CONTRACT NUMBER
W81XWH-10-1-0614

5b. GRANT NUMBER

5c. PROGRAM ELEMENT NUMBER

6. AUTHOR(S)
Sai Yendamuri, MD

E-Mail: Sai.Yendamuri@RoswellPark.Org

5d. PROJECT NUMBER

5e. TASK NUMBER

5f. WORK UNIT NUMBER

7. PERFORMING ORGANIZATION NAME(S) AND ADDRESS(ES)
Health Research, Inc.
Roswell Park Cancer Institute Division
Elm and Carlton Streets
Buffalo, NY 14263

8. PERFORMING ORGANIZATION REPORT NUMBER

9. SPONSORING / MONITORING AGENCY NAME(S) AND ADDRESS(ES)
U.S. Army Medical Research and Materiel Command
Fort Detrick, Maryland 21702-5012

10. SPONSOR/MONITOR'S ACRONYM(S)

11. SPONSOR/MONITOR'S REPORT NUMBER(S)

12. DISTRIBUTION / AVAILABILITY STATEMENT
Approved for Public Release; Distribution Unlimited

13. SUPPLEMENTARY NOTES

14. ABSTRACT

The primary aim of this project is to laser microdissect stage I lung cancer samples, perform microRNA profiling of the epithelial and stromal components and develop component specific signatures of prognosis. This report summarizes the work performed on the project so far. Data analyses indicate that there is a significant difference in the microRNA expression profile of epithelia and stroma in NSCLC tumors and that these profiles have prognostic import with stroma having more prognostic value than epithelia. Also, the fold changes seen along with variability of in-situ hybridization (ISH) measurements do not support pursuing the development of prognostic ISH biomarkers. Based on the data, two microRNAs were chosen for further study. miR-372 overexpression makes cell lines more aggressive with increased migration and invasion. miR-146b was chosen as the stromal miRNA for further study. A no-cost extension was granted to complete these experiments.

15. SUBJECT TERMS
Lung cancer; microRNA, prognosis, biomarkers, laser microdissection

16. SECURITY CLASSIFICATION OF:			17. LIMITATION OF ABSTRACT	18. NUMBER OF PAGES	19a. NAME OF RESPONSIBLE PERSON
a. REPORT	b. ABSTRACT	c. THIS PAGE			19b. TELEPHONE NUMBER *(include area code)*
U	U	U	UU	18	USAMRMC

Table of Contents

	Page
Introduction...……..……...	**4**
Body.....……	**4**
Key Research Accomplishments…….……	**16**
Reportable Outcomes……	**17**
Conclusions……	**17**
References…….	**17**

INTRODUCTION

Even stage I lung cancer patients have an unacceptably high rate of recurrence (~35%)[1]. A prognostic assay can help identify patients for intensified treatment such as adjuvant chemotherapy. Our previous data has demonstrated the potential of microRNA profiling of whole tumors to prognosticate early non-small cell lung cancer (NSCLC)[2]. However, some of the prognostic "signal" may be masked by varying composition of whole tumors with respect to their epithelial and stromal components. In this project, we intended to perform laser capture microdissection of lung cancer specimens to separate out the epithelial and stromal components of tumors and perform microRNA profiling of these separate components to try to improve microRNA-based prognostic assays for NSCLC, and to identify the localization (non-cancerous stromal vs. cancerous epithelial) of the prognostic signals of the biomarker microRNAs. In addition, we sought to study the biological import of two prognostic, stromal- and epithelial component-associated microRNAs.

In this final report for the grant award, the works that were performed for the above goals and their findings are summarized under italicized statements of the four Tasks in the Statement of Work for the award.

BODY

Task 1: To identify epithelium- and stroma- specific miRNA signatures for the prediction of recurrence after resection of early stage NSCLC.

1a. Laser capture micro-dissection of samples*: Formalin-fixed paraffin embedded tissue blocks for the 77 samples identified for the study will be retrieved from the tissue archives of the Pathology Resource Network Core at Roswell Park. Laser capture micro-dissection of these specimens will be performed to separate the epithelial from the stromal components. RNA will be extracted from these components to assure at least 200 ng of total RNA is obtained from each component. An IRB approved protocol for access to this tissue is already in place.*

1b. MicroRNA microarray of samples*: All 154 specimens (77 epithelial and 77 stromal) will be assayed by microRNA microarray. RT-PCR will be performed for six random miRNA will on 10 samples to confirm good correlation across both platforms.*

1c. Analysis of microarray data and development of classifiers*: The miRNA expression of whole tumors (already available) will be compared to that of the epithelial and stromal components to assess for systematic differences. Each set will then be assessed for its ability to prognosticate lung cancer.*

1a.1. Laser capture micro-dissection of samples: Optimization of methods

In this phase of the study, a number of variables were examined for their effect on the yield of microRNAs in samples obtained from formalin-fixed paraffin-embedded tissues by laser microdissection. The observations that were obtained were found to be of value for the efficient isolation of microRNAs from microdissected formalin-fixed tissues with a flexible workflow for the next phase of the study (further below).

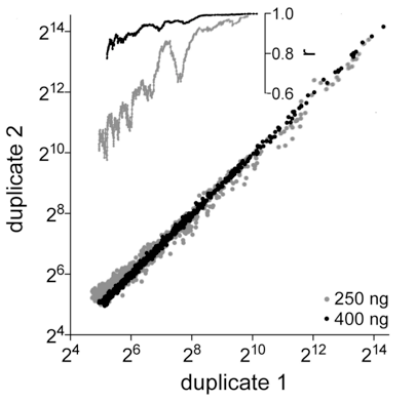

Figure 1. Microarray signal values (dots) and inter-duplicate Pearson correlation coefficient, r (lines) for 747 microRNAs measured in duplicate using 250 (grey) or 400 ng (black) of RNA prepared from an LMD sample. A rolling window of width 99 along the X axis was used for calculating value of r at the mid-window abscissa.

In our preliminary data submitted in the proposal, the feasibility of microRNA profiling using laser capture microdissected specimens was established using 100 ng input RNA from a few samples with quantification of the RNA being performed by absorbance at 260 nm using the Nanodrop™ spectrophotometry device. However, before embarking on this major project, we sought to optimize variables that may influence miRNA quantification by microarray and to set up a feasible workflow to enable a reasonably high throughput processing of tissue.

One of the first variables tested was the amount of total RNA input needed for reproducible microarray quantification. In order to do this, 250 or 400 ng of the same RNA sample obtained by LCM was labeled with the Hy3 dye and hybridized in duplicate to miRCURY™ (Exiqon®, Denmark). With both amounts, ~56% of the 1291 microRNAs detectable by the microarrays were identified as expressed. Not surprisingly, microarray signals were stronger with higher RNA input (Figure 1). However, inter-duplicate correlation analyses clearly demonstrated microRNA quantifications were more accurate and less noisy when 400 ng of RNA was used. As demonstrated in the inset in Figure 1, reliable quantitation of a much greater number of microRNAs are found with 400 ng than with 250 ng, a finding not apparent when only the number of microRNA considered expressed is measured. This finding was clearly important to our proposed project.

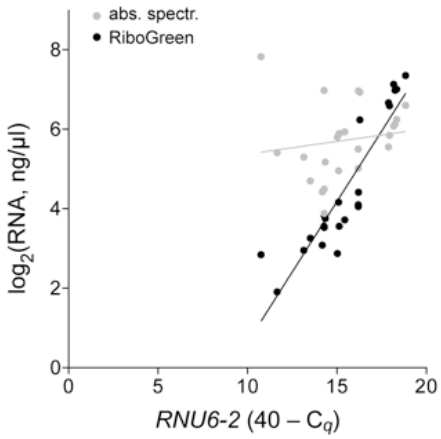

Figure 2. Scatter-plots of RNA concentration and RNU6-2 measurements of RNA from dissectates of formalin-fixed tissue sections.

While an increase in total RNA input can be simply increased by an increase in the total area of dissection performed, a fourfold increase in the area of dissection is not practical, given that, in some specimens, 6-8 hours of dissection is required to obtain 100 ng of total RNA. Therefore, we evaluated individual variables affecting RNA yield from microdissectates and in a series of experiments to boost our yield. A summary of the results from our experiments is summarized below.

1) RNA yield is best estimated by Ribogreen assay measurements and not by absorbance at 260 nm. This conclusion was based on measurement of correlation between RNU6-2 levels and RNA quantification performed by either method in 23 dissectates (Figure 2). The Pearson correlation coefficient was 0.91 ($P<0.01$) for Ribogreen and statistically not significant ($P=0.15$) for absorbance.

2) Comparison of the use of H&E (hematoxylin and eosin) and CV (cresyl violet) demonstrated that RNA extracted after CV stain was 2-3 times higher than that with H&E. However, recognition of key histological elements was better with H &E and

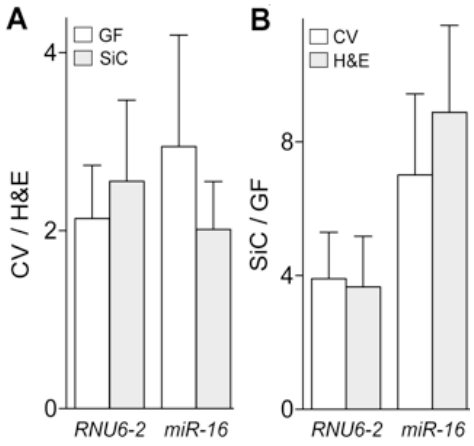

Figure 3. Yields with cresyl violet (CV) stain relative to hematoxylin and eosin (H&E) for glass fiber (GF) and silicon carbide (SiC) columns (A), and with SiC relative to GF columns for both stains (B) are plotted as means with their standard errors for n=3.

therefore, a decision to continue to use H & E was made (Figure 3).

3) Comparison of the use of glass fiber based columns and silica carbide based columns demonstrated 4-7 times higher yield with silica carbide columns when compared to the glass fiber columns, an impressive difference (Figure 3).

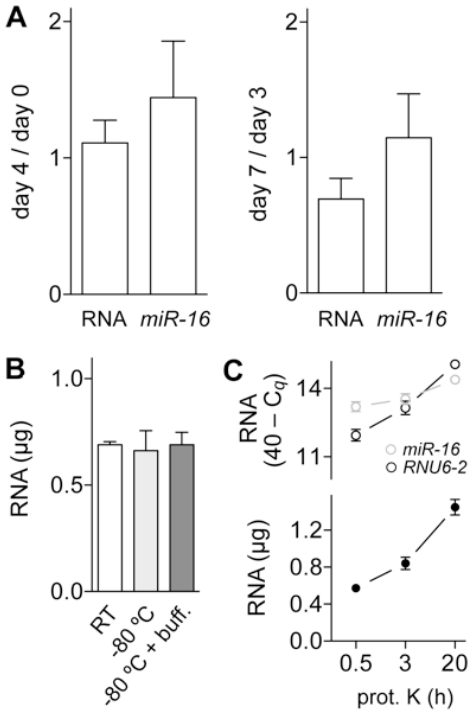

Figure 4. Effect of age of slides and dissectates, and proteinase K treatment duration on RNA yield A. Total RNA and miR-16 yields from laser microdissectates from three tissues prepared from four or seven day-old slides relative to zero or three day-old ones, respectively. B. Total RNA yield from identical laser dissectates from zero day-old slides stored in duplicate at room temperature (RT), or at -80 ºC with or without buffer (buff.) for a day. C. Total RNA yield (filled circles) and levels of RNU6-2 (black empty circles) and miR-16 (grey empty circles) from identical dissectates treated in triplicate with proteinase K (prot. K) for 0.5, 3 or 20 h. Means and their standard errors are plotted. Log_2-transformed RNU6-2 and miR-16 levels were determined from quantification cycle (C_q) values obtained in reverse transcription-PCR assays. Total RNA was quantified by RiboGreen assay. Hematoxylin-eosin was used as the histologic stain, and silicon carbide columns were used for RNA isolation.

4) It is often difficult to prep slides and dissect them the same day. While this delay decreases the quality of mRNA when frozen sections are used, such an effect may not exist with FFPE samples, such as those used in our experiments. We compared the RNA yield in samples cut on day 0, day 3 and day 7 and did not find significant differences in RNA yield (Figure 4). Similarly, after dissection, storage at room temperature, -80 ºC either in a dry state or in the tissue lysis buffer did not affect RNA yield.

One of the important steps involved in sample processing involves proteinase K digestion. RNA yield increases 1.5 fold when digestion time is increased from 15 min at 55 C to 3 hours. Further this yield increases by 1.7 times when the treatment time is extended from 3 to 20 hours (Figure 4).

Estimation of RNA yield by area of dissection: RNA yield from dissection can vary a great deal and it is important to have an idea of how much dissection is required to obtain a given amount of RNA. Based on the first 27 cases, we have determined that, using our protocol, an average yield of 84 ng of total RNA can be obtained from 1 mm^2 of a dissectate.

As demonstrated above, a number of experiments were performed to optimize our protocol before dissection of valuable human specimens was even started. This is due to the paucity of published data and protocols that could be readily used for our project. While this has delayed our project modestly, the information gained from our protocol optimization is valuable to the scientific community in general. This data has been published in a peer-reviewed research article (see *Reportable Outcomes* below).

1a.2. Laser capture micro-dissection of samples: Dissection of 77 pathologic stage I NSCLC tissues

Epithelial and stromal components of 8 um-thick hematoxylin-eosin-stained formalin-fixed (paraffin-embedded) sections of pathologic stage I NSCLC were dissected using Leica® (Buffalo Grove, IL) LMD6000 laser capture microdissection system in the Department of Pathology at Roswell Park Cancer Institute. The dissection was performed by one of our laboratory members or a Department of Pathology personnel under the guidance of a pulmonary pathologist. Microdissection for a total of 82 tumor blocks was performed during a period of ~18 months. This required a total of ~132 microdissection sessions, with many tumor blocks requiring multiple sessions for adequate RNA yield. Typically, a

microdissection session lasted 2.5-3 hours. Microdissectates were kept at -80 ºC until RNA extraction. RNA was extracted from the microdissectates after overnight proteinase K treatment using silicon carbide matrix-containing spin columns (FFPE RNA Purification kit, Norgen-Biotek®, Thorold, ON, Canada; cat.# 25300). DNAse I treatment was not performed during or after the RNA isolation procedure. RNA was eluted in water and quantified using 'low range' Ribogreen assay using QuantIt™ Ribogreen dye (Invitrogen®, Carlsbad, CA). RNA isolates from multiple microdissection sessions were pooled for many tumor cases to achieve the 350 ng amount that was used for global microRNA profiling.

1b. MicroRNA microarray of samples

MicroRNA expression profiling of microdissectate RNAs was performed as a commercial service by Exiqon® (Vedbaek, Denmark) during May-September 2012. Exiqon®'s seventh generation miRCURY™ locked nucleic acid microarrays, with signal detectability over 5 orders of magnitude, were used (product number 208500). For each microdissectate RNA sample, 350 ng of an RNA sample was labeled with the Cy3-like Hy3™ (Exiqon®) green fluorescent dye, and, along with 350 ng of reference RNA (Ambion® (human universal reference RNA made by pooling components of FirstChoice™ human total RNA panel (Ambion®, Austin, TX; product# AM6000) labeled with Cy5-like Hy5™ (Exiqon®) red fluorescent dye, was hybridized to a microarray. The AM6000 RNA was provided by Exiqon®. All RNA samples were spiked with 62 artificial small RNAs before labeling; the microarray has probes to detect the artificial RNAs. Locked nucleic acid-containing DNA oligonucleotide probes are printed on the array in quadruplicate spots of 100 µm diameter with 185 µm inter-spot distance in 36 sub-arrays. Hy3™ 'guide-spots' present on the arrays. miRBase version 19-based annotations of the arrays suggest that a total of ~1,940 probes target 20 human non-microRNA small RNAs like RNU6B (20 probes), 23 human miRPlus™ (Exiqon®) mature microRNAs (23 probes), and ~1,920 human mature microRNAs that are recorded in the miRBase database (~1,900 probes). Thirty of the probes on the array platform that recognize human mature microRNAs target multiple microRNAs (72 total; 2-6 per probe), and a few of the microRNAs recognized by the 30 probes are also targeted by a second probe on the array platform. The array platform also has probes that target microRNAs of mouse, rat and a few viruses. Arrays also have probes for artificial 'spiked-in' RNAs. In total, 170 microarrays were used.

1c. Analysis of microarray data and development of classifiers

Raw microarray data was processed similar to what has been described previously by us[2]. Briefly, within-array and between-array normalizations used the global Loess and quantile methods. Log_2-transformed, normalized microarray signals were used for final analyses that included those for inter-replicate correlation, unsupervised hierarchical clustering, histology-, recurrence- or stromal/epithelial component-based differential expression, etc.

Data obtained with the microarray experiments were of technically good quality for 153 of the 170 microarrays; i.e., for a total of 77 epithelia and 76 stroma from a total of 79 lung cancer cases. For 5 cases, good data was obtained only for either epithelia or stroma. Analysis of non-log-transformed Hy3™ expression values after 'quantile' within-array normalization and probe-filtering (so signals

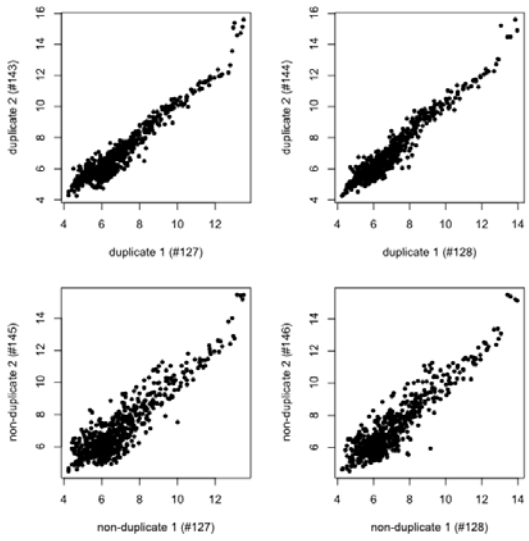

Figure 5. Correlation between microRNA measurements obtained for two pairs of technical replicates (above) and two pairs of non-replicates. Normalized, log_2-transformed expression values for 595 microRNAs are plotted in each scatter-plot.

from a probe in >1/8th of the 155 samples are >3x within-array probe-set summarized 'empty' spot values) suggested that expression of a total of 595 microRNAs was reliably quantified for these samples. The two pairs of technical replicate samples showed good correlation for microRNA expression measurements (Figure 5). A heat map of the experiment with unsupervised clustering is depicted in Figure 6.

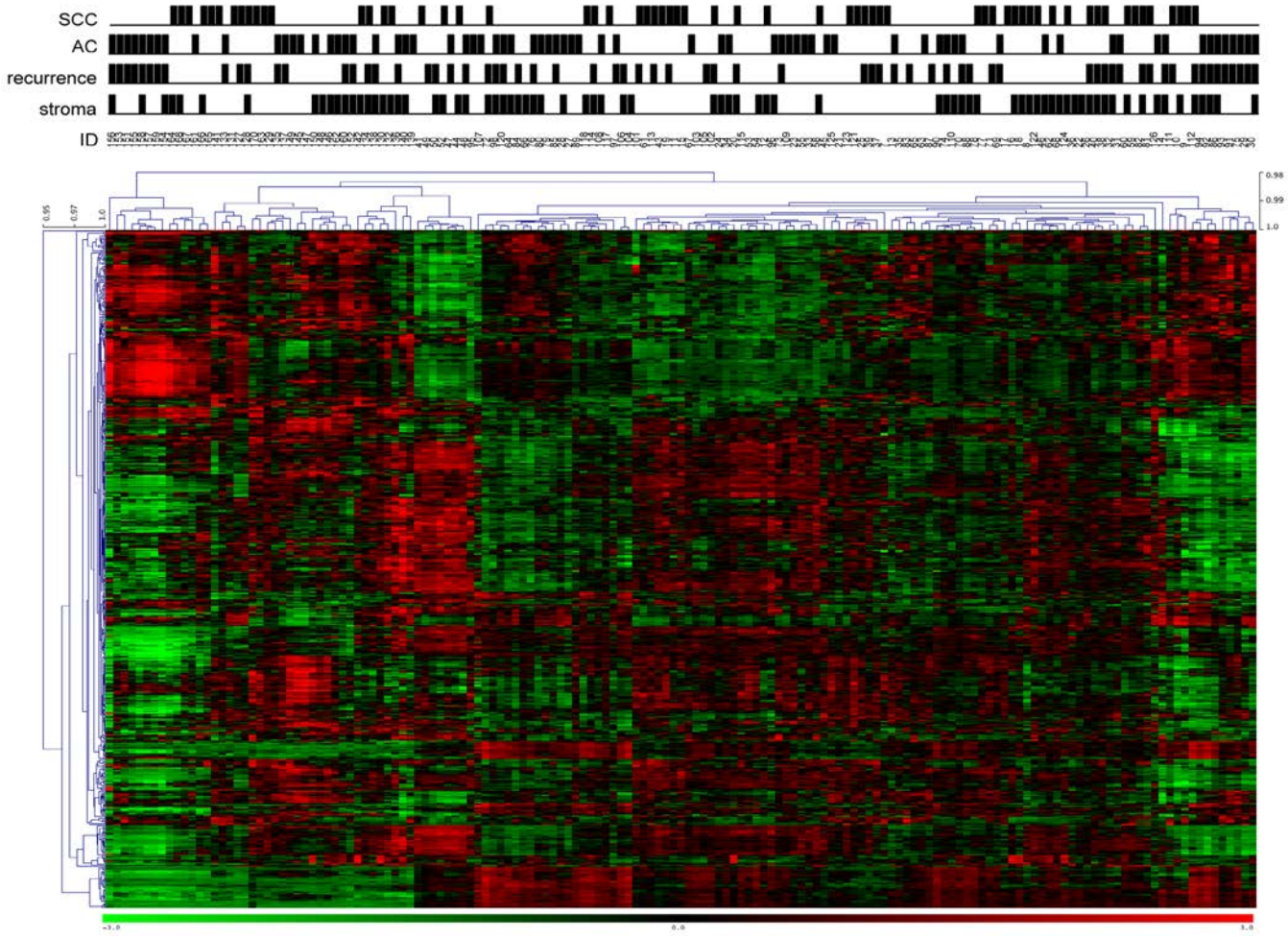

Figure 6. MicroRNA expression heat map, with its pseudo-color scale underneath, depicts Z-scaled $\log_2$-transformed normalized microarray signal values for 77 epithelial and 76 stromal samples of 79 NSCLC cases. The sample (top) and microRNA (left) dendrograms are shown next to the heat map. Scales next to the trees indicate node heights. Graphs at the top of the figure indicate if stromal tumor component, recurrence, and adenocarcinoma (AC) or squamous cell carcionoma (SCC) histology of cancer. Sample identities (ID) are also indicated. A total of 595 microRNAs were used to generate the heat map and dendrograms using uncentered Pearson correlation as distance metric and average inter-cluster distances.

The microRNA expression measurements obtained by microarray were partially validated by RT-PCR. Ten randomly picked microRNAs were quantified in a total of 28 randomly picked RNA isolates of the dissectates. For RT-PCR, commercial, stem-loop RT primer-based Taqman™ microRNA assays from Life Technologies® were used. Quantification cycle (Cq) values were normalized using that of the SNORD44 small nuclear , housekeeping RNA. As shown in Figure 7 for four of the tested microRNAs, good correlation between measurements obtained by microarray and RT-PCR were noted for all tested microRNAs.

Several preliminary analyses were then performed to explore the data further. Two primary questions were asked: 1) Are there differences between epithelial and stromal components and 2) Are component specific microRNAs differentially expressed between patients with and without recurrence? For all analyses, log-transformed values were used with limma's moderated t statistics with Benjamini-Hochberg correction for FDR < 5%. P<0.05 was considered statistically significant.

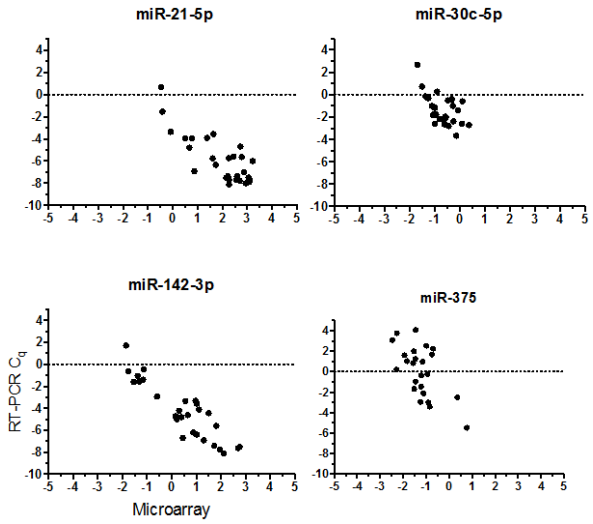

Figure 7. Correlation between microRNA measurements obtained for 28 RNA samples by RT-PCR and microarray. RT-PCR data is normalized against intra-sample SNORD44 measurements whereas microarray data are quantile-normalized.

(1) Epithelia (n=77) vs. stroma (n=76), unpaired, disregarding histology or recurrence: 227 of 587 probes (233 of 595 microRNAs) were differentially expressed. Five each probes with up- or down-regulation with highest degree of fold-change:

MicroRNA	*epithelia/stroma (log2)*
miR-205-5p	0.87
miR-200b-3p	1.01
miR-200a-3p	1.15
miR-200c-3p	1.48
miR-141-3p	1.62
miR-143-3p	-1.32
miR-199a-5p	-1.26
miR-4539	-1.23
miR-142-3p	-1.19
miR-199a-3p/miR-199b-3p	-1.16

(2) Epithelia (n=77) vs. stroma (n=76), paired (74 epi.-str. pairs), disregarding histology or recurrence: 373 of 587 probes (380 of 595 microRNAs) differentially expressed. Five each probes with up- or down-regulation with highest degree of fold-change:

MicroRNA	*stroma/epithelia (log2)*
miR-141-3p	-1.63
miR-200c-3p	-1.48
miR-200a-3p	-1.17
miR-200b-3p	-1.04
miR-205-5p	-0.88
miR-199a-3p/miR-199b-3p	1.15
miR-142-3p	1.16
miR-4539	1.21
miR-199a-5p	1.26
miR-143-3p	1.33

(3) Recurrence (n=34) vs. no recurrence (n=42), using stromal expression, disregarding histology. 15 of 587 probes (15 of 595 microRNAs) differentially expressed. Five each probes with up- or down-regulation with highest degree of fold-change:

MicroRNA	*recurrence/no recurrence (log2)*
miR-4539	-0.75
miR-4513	-0.66
miR-4497	-0.50
miR-711	-0.43
miR-3196	-0.43
miR-106a-5p	0.27
miR-17-5p	0.35
miR-200a-3p	0.42
miR-200c-3p	0.59
miR-141-3p	0.62

(4) Recurrence (n=33) vs. no recurrence (n=44), using epithelial expression, disregarding histology: No differentially expressed genes at $P<0.05$. at $P=0.06$, 31 probes are considered differentially expressed.

The main conclusions of these analyses were:

1) The epithelial and stromal components of tumors are significantly different in terms of microRNA expression.
2) Most prognostic information arises from the stroma.
3) Fold-change microRNA expression differences obtained from component-specific microRNA profiling are in the same range as that of whole tumor microRNA profiling.

Task 2 : To develop a miRNA in situ hybridization (ISH) assay with performance characteristics comparable to a miRNA microarray for prediction of recurrence after resection of early stage NSCLC using epithelium-specific data obtained with Task 1.

2a. In situ hybridization assay assessment for ten candidate miRNAs*: Ten miRNA ISH assays will be performed on 20 samples randomly selected by stratified sampling from the patient cohort of 77 samples described above and used for Specific Aim 1 and expression scores generated. Only those assays with robust features, showing good correlation with relapse will be explored further. In line with our prediction goals, a refined signature of miRNAs will be composed of only miRNA predictors that are selected with greater than 30% probability.*

2b. In-situ hybridation of three to six miRNA on the remaining 57 samples*: Three-six miRNAs that pass through this first screening step will be used to perform ISH on the remaining 57 samples. Data from the expression scores derived from these hybridizations will be used to predict outcome. Predictions will be compared to predictions using microarrays. A non-inferiority analysis will be performed.*

In this phase of the study, we found that in situ hybridization (ISH) is not a good technique for the development of robust prognostic biomarkers for NSCLC.

As with all in-situ hybridization methods, microRNA in-situ hybridization has proven to be technically challenging. However, over six months, we had consistently been successful in performing this technique in our laboratory. Qualitatively, a summary of our observations are:

1) For miRNA in-situ hybridization to work well, the miRNA has to be expressed at a reasonably high level. Therefore, this technique does not work well for miRNAs expressed at a low level, but may be detectable by microarray. For example, despite multiple attempts at ISH, this was not successful using probes for miR-375, a microRNA that is expressed at a low level.

2) Even for robustly expressed microRNAs, there is significant experimental variation in the strength of signal obtained. To quantitatively demonstrate this, ISH using probes against miR-205 were performed in triplicate using an adenocarcinoma (AC) and a squamous cell carcinoma (SCC). After confirmation of successful hybridization, images were acquired at 20X magnification without a light filter at an acquisition time of 1/13 sec. JPEG images obtained were analyzed using ImageJ (version1.41n). The RGB channel was split and the red channel's signal was used for analysis. After background subtraction, the image was made binary and particles analyzed. Measurements of the miR-205-hybridized slides were normalized to their corresponding scramble-control hybridized slides. Triplicate measurements are summarized in Figure 8.

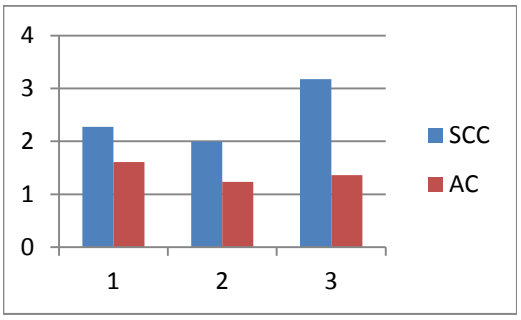

Figure 8. miR-205 expression as measured by ISH using triplicate slides (1-3) of one each of SCC or AC tumors. SCC= squamous cell carcinoma; AC = adenocarcinoma.

In other experiments conducted by our group, we know that miR-205 is expressed an average of 65-fold higher in SCCs compared to ACs. While the figure above does show that measurements of miR-205 are higher in SCC than those with AC, the differences are greatly muted. Even more concerning is the fact that the standard deviation of these measurements are ~25% for the triplicate slides when performed at the same time together. We also observe that when the slides are hybridized on different days, this variation is amplified several-fold.

Observations shown above are consistent with data published since this proposal was written. Nielsen et al.[3] show the potential of using a highly automated system of quantifying ISH for use as a biomarker. However, they note that the coefficient of variation (CV) of the same measurement in different areas of a slide is 125%. For specific derived values, this was 67-71%. Therefore, any application aiming to use this method can only aim to detect miRNA levels that are several-fold different in comparison tissues. At least a portion of this variation comes from tumor heterogeneity. This issue was observed by Hanna et al. as well[4]. In this comprehensive study, the investigator found that the correlation between multiple histospots from the same tumor demonstrate correlation coefficients ranging from 0.4-0.6 vs. immunohistochemistry where the same measurements are in the 0.6-0.8 range.

Therefore, we concluded that ISH has limited reproducibility and is not suitable for biomarker development unless the fold changes expected are high. In our preliminary data submitted for this proposal[2], among the microRNAs deemed to be the most robust biomarkers for prognosis, the highest fold change seen was for miR-200b* (0.71). Therefore, we inferred that ISH is not a good technique for the development of prognostic biomarkers for NSCLC. Given the findings with Task 1, we decided not to pursue the ISH-based line of investigation any further.

Task 3: To study the role of two miRNAs predicting prognosis in regulation of the phenotype of lung cancer.

3a. Further higher-level analyses of the microarray data will be performed to select two microRNAs *suitable for further functional study.*

3b. Creation of stably transfected cell populations*: The selected miRNAs will be cloned into transfer vectors, lentivirii generated and used to develop stably transfected populations.*

3c. Cell line experiments to evaluate phenotype: *Cell line assays as described in the methods section will be performed in triplicate to assess for alteration in phenotype secondary to overexpression of the specific miRNAs.*

3d. Xenograft formation assays: *Xenograft formation assays will be performed here in triplicate. An existing IACUC protocol will be amended to perform these experiments. As these experiments start in year 3, there is ample time to amend the existing protocol.*

3e. Identification of miRNA targets*: 3'UTR reporter assays will be performed to identify bonafide miRNA targets to explain the altered phenotypes.*

3f. Assessment of the role of miR-146b in altering macrophage differentiation: miR-146b constructs will be used to study the role of M1 to M2 macrophage conversion as described above

3a. Further higher-level analyses of the microarray data will be performed to select two microRNAs

In this phase of the study, the effect of overexpression of two epithelium-enriched NSCLC-prognostic microRNAs, miR-372 and miR-486 on the cancer phenotype of lung cancer cells was examined. As described below, a significant effect of miR-372 overexpression, which correlated with its prognostic value for NSCLC, was noted.

Selection of the epithelial microRNAs for further biological examination was performed in the following fashion:

1. The microRNAs with the greatest difference between patients with and without recurrence in the epithelial components were identified.
2. This list was refined further based on other microRNA profiling studies to select the top prognostic microRNAs and ranked accordingly.
3. A literature search was performed to identify those microRNAs whose biological role has already been elucidated and these were excluded from further study.

Based on the above steps, microRNAs miR-372 and miR-486 were selected.

3b. Creation of stably transfected miR-372/-486-overexpression NSCLC cell-line populations

The precursor DNAs for miR-372 and miR-486 were cloned into transfer vectors, and lentivirii generated and used to develop stably transfected populations of A549 and H460 cell-lines that overexpressed these microRNAs. The microRNAs were expressed from the 3' UTR of a green fluorescent protein (GFP) RNA that acted as the 'host' gene for the inserted precursor microRNAs. During this time, a publication elucidating the role of miR-486 in NSCLC cell-lines was published[5]; therefore, the study of this miR-486 was stopped. The experiments and analyses of miR-372 was continued. The miR-372-overexpressing H460 population was found to lose overexpression of the microRNA over time (Figure 9), and further work using this cell-line was

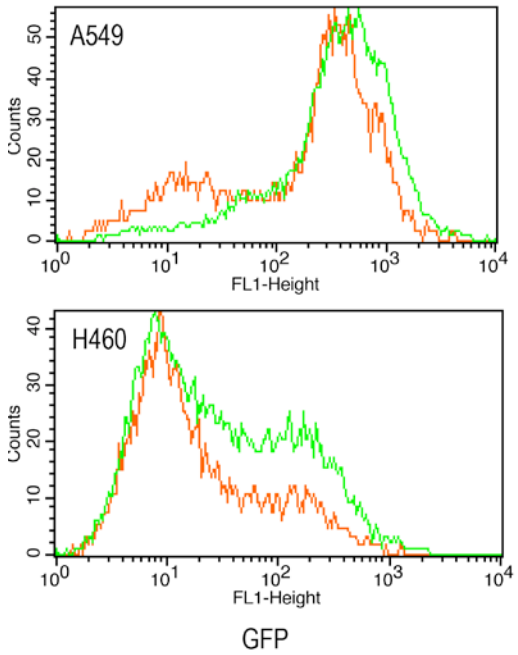

Figure 9. GFP expression in stable populations of miR-372-overexpressing A549 and H460 cells overtime. Flow cytometry profiles of GFP expression at two time-points (*green* and *red*, two weeks after green) are shown.

discontinued. The overexpressing A549 cell-line over-expressed miR-372 by ~9 log2 units relative to control A549 cells that were generated using the empty, GFP-expressing construct without a precursor microRNA insert.

Effect of miR-372 over-expression on proliferation, migration and invasiveness, adherent colony formation, and xenograft tumor formation of A549 lung cancer cells was examined by comparing against control cells a stably-transduced population of the cell-line that was engineered to over-express the microRNA. Microarrays were used to identify the global effect of miR-372 over-expression on gene expression in the cells. Targeting of specific gene transcripts by miR-372 was assessed by quantifying the effect of microRNA overexpression on target RNA and protein levels and on the activity of a synthetic luciferase reporter construct bearing a miR-372 target site.

3c. Cell line experiments to evaluate phenotype

Compared to control, miR-372-overexpressing cells proliferated faster, with a higher percentage of the cells in S phase of cell cycle (Figure 10). The cells had a higher migration rate and an increased collagen matrix invasibility (Figure 10).

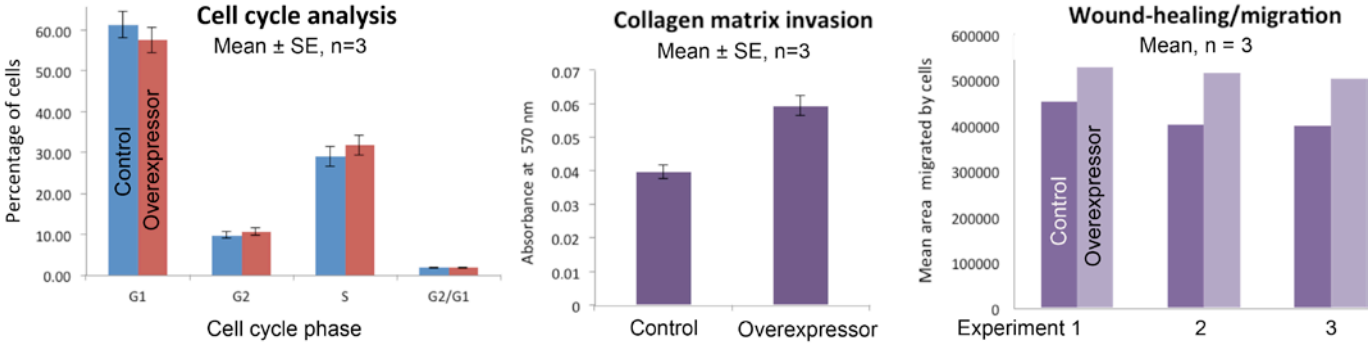

Figure 10. Cell cycle, collagen matrix invasion, and migration assays of control and miR-372 overexpressing A549 cell-line populations.

3d. Xenograft formation assay

Compared to control, miR-372-overexpressing cells had enhanced adherent colony formation ability in vitro and generated larger xenograft tumors in SCID mice (Figure 11).

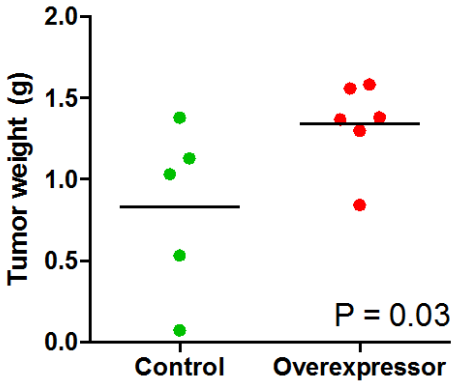

Figure 11. Weights of xenografts generated in female SCID mice by subcutaneous injection of 0.5 million control or miR-372-overexpresing A549 cell populations. P value is for one-tailed standard t test. Six mice each were injected for both cell types, but one mouse did not develop a tumor. All mice were injected concurrently.

3e. Identification of miRNA targets; 3'UTR reporter assays will be performed to identify bonafide miRNA targets to explain the altered phenotypes

Microarray analysis for gene expression of control and miR-372-overexpressing A549 populations (n=3 each) using Affymetrix® GeneChip™ Human Gene 2.0 ST arrays was used to identify possible target mRNAs of miR-372. MiR-372 overexpression altered the expression of 1,186 genes. Of these, 147 had reduced expression (suggesting possible targeting by miR-372). Additionally, the miRWalk database[6] of microRNA targets was queried to obtain a list of 8,252 validated targets (genes) for miR-372. By examining these lists, and existing literature on miR-372-targeted genes, and

genes associated with prognosis of NSCLC, we identified CA12 (carbonic anhydrase 12) gene, whose transcript encodes for a carbonic anhydrase and bears a predicted miR-372 target site, as a possible miR-372 target of importance that has not been studied by others. Many other genes of relevance to lung cancer were also identified by this strategy; however, their targeting by miR-372 was found to have been studied by others in the past. These genes included those in the P53 pathway[7].

Targeting of CA12 mRNA by miR-372 was confirmed using a microRNA target reporter assay (Figure 12) and by noting a reduction in CA12 RNA and protein levels consequent to miR-372 overexpression.

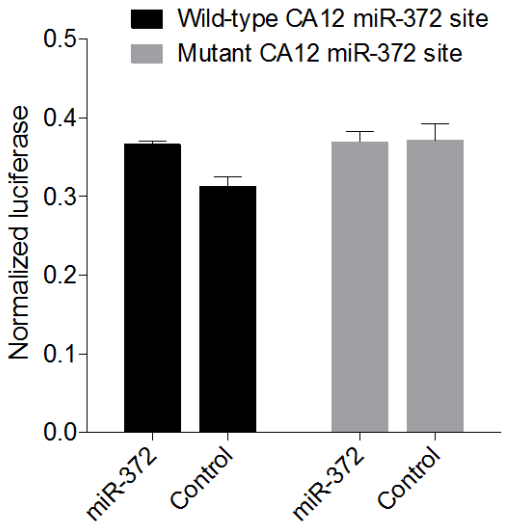

Figure 12. The predicted miR-372-binding site of CA12, with or without a single nucleotide mutation in the microRNA seed region, was cloned in the 3'UTR of firefly luciferase. The luciferase construct was co-transfected in A549 cells with a constitutionally expressed Renilla luciferase construct along with control or miR-372 precursors RNAs. Firefly luciferase activity normalized to the Renilla luciferase activity in the transfectant cell lysates was measured after ~24 h. Mean ± SD for n=3 are plotted.

These findings indicate that miR-372 enhances the malignant nature of lung cancer cells and provides an explanation for the association of the microRNA's expression level with survival and relapse in non-small cell lung cancer. The identification of CA12 as a miR-372 target is consistent with the observation that reduced CA12 level is associated with poor survival and higher rate of relapse in lung cancer[8,9].

3f. Assessment of the role of miR-146b in altering macrophage differentiation

In the analysis of the microRNA expression in the epithelial and stromal components of the lung cancer tissues, a significant number of microRNAs were seen to be expressed in the two compartments. Of the epithelial microRNAs, miR-372 was studied as described above. We also decided to study biological role of a stromal microRNA. Based on our component profiling experiments, several potential candidates were available for this. Of these, we chose miR-146b for further study based on the following reasons:

1) miR-146b has been shown, by us as well as others, to be very strong prognostic marker.[2,10].
2) We have demonstrated convincingly that miR-146b does *not* alter epithelial lung cancer cells[11].
3) miR-146b is very strongly expressed in macrophage-monocyte lineages compared to all other tissues[12].

Based on the data above, we hypothesized that miR-146b influences the differentiation of M1 to M2 macrophages. To test this hypothesis, we used a well published model that used in vitro differentiated and polarized macrophages generated from monocytes that have been isolated from peripheral blood[13]. Specifically, anti-CD14 antibody-conjugated microbeads (Miltenyi Biotec®) were used to isolate CD14+ monocytes from peripheral blood mononuclear cells that had been collected using Ficoll™ gradient from blood retained in Accel Trima™ leucoreduction filters that had been used for collection of platelets from healthy blood donors. In this model, monocytes are first differentiated into M0 or basal macrophages by culture on plastic dishes in the presence of monocyte colony stimulating factor (MCSF) for seven days. The M0 macrophages are then exposed to interferon-gamma (IFNg) and lipopolysaccharides, or interleukin 4 (IL-4) for 18-24 hours to respectively differentiate them into M1 or M2 macrophages. Polarization of the macrophages was assessed by flow cytometry for cell surface markers such as CD206 (MRC1) as well as by quantitative RT-PCR for expression of genes such as CCL2, CCL19, and NOS2.

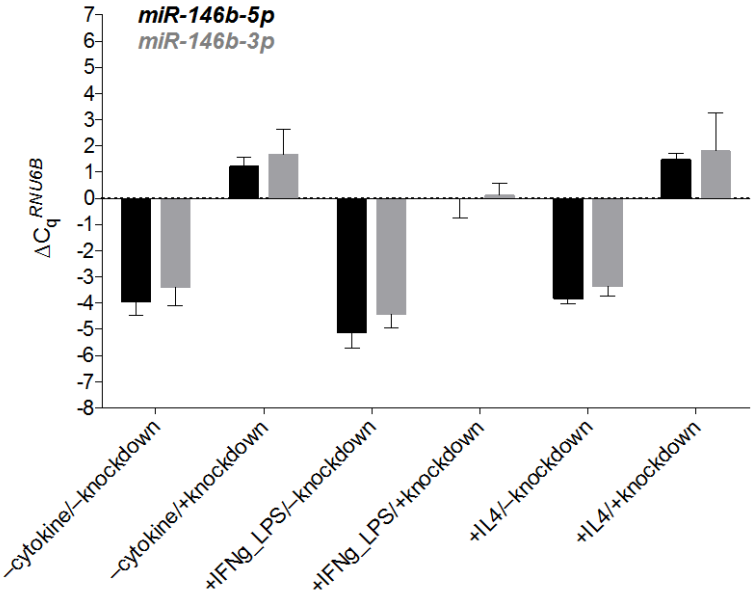

Figure 13. Knock-down of miR-146b-5p or -3p in M0 macrophages by transfection of antisense oligos against the microRNAs 24 hours before polarization of the macrophages to M1 (with IFNg and LPS) or M2 (with IL4) macrophages. Control cells were not treated with any cytokine. MicroRNA levels were quantified by RT-PCR and normalized against that of RNU6B. The Y axis indicates inverse values of normalized, $\log_2$ microRNA levels. Mean ± SE for n=3.

For microRNA engineering, precursor miR-146b microRNA, in case of overexpression, or antisense nucleic acids (Exiqon® miRCURY™, and Life Technologies® miRVana™ microRNA inhibitors), in case of knock-down, were chemically transfected using RNAiMax™ reagent (Life Technologies®) 24 hours before induction of polarization. The antisense oligos were specific to either of the two mature miR-146b microRNAs, miR-146b-5p and -3p. Engineering of microRNAs in >80% of cells was confirmed by fluorescence microscopy and quantitative RT-PCR that showed at least 8-fold change in microRNA levels compared to scrambled control nucleic acids (example data in Figure 13).

The effect of knocking down or overexpressing miR-146b in macrophages on subsequent cytokine-induced M1 or M2 polarization was studied by examining the cells using flow cytometry and RT-PCR for M1/M2 macrophage markers such as CD23 (FCER) and CD206 (MRC1) that are expressed less in M1 compared to M2, and CCL2 and CCL19 that are expressed more. Through these assays, we were unable to discern any significant effect of miR-146b expression in macrophages on their M1/M2 polarization. Representative data for an overexpression experiment that used RT-PCR is shown in Figure 14.

Task 4: Collation of results and manuscript writing.

One peer-reviewed research article based on the findings obtained in this research project has been published so far:

1. Patnaik SK, Kannisto E, and Yendamuri S. Factors affecting the yield of microRNAs from laser microdissectates of formalin-fixed tissue sections. *BMC Research Notes*. 5(1):40, 2012

We are currently preparing manuscripts and aim to publish two additional peer-reviewed research articles based on the findings obtained in this research.

We have submitted the following abstract for peer-reviewed consideration for presentation at the International Association for the Study of Lung Cancer's 16th World Conference on Lung Cancer in Denver, CO, during 6-9 September 2015; a decision is expected by June 2015:

1. Patnaik SK, Mallick R, Kannisto E, Bshara W, and Yendamuri S. MicroRNA expression in epithelial and stromal components of early-stage non-small cell lung tumors.

These research presentations will duly acknowledge the primary support provided by this research grant. No patent that is based on the findings obtained in this research project was or will be applied for.

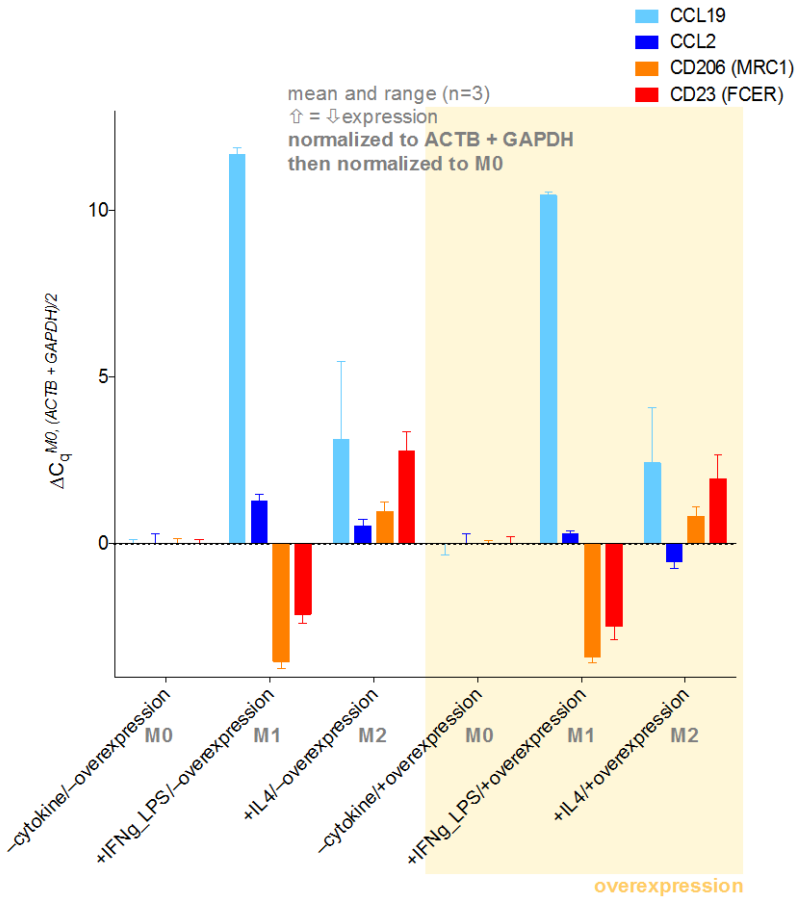

Figure 14. Effect of miR-146b overexpression on M1 and M2 macrophage marker gene expression. Overexpression of miR-146b microRNAs in M0 macrophages by transfection of precursor miR-146b RNA 24 hours before polarization of the macrophages to M1 (with IFNg and LPS) or M2 (with IL4) macrophages. Control cells were not treated with any cytokine. Gene expression levels were quantified by RT-PCR and normalized against that of actin (ACTB) and GAPDH. The Y axis indicates normalized, $\log_2$ gene expression levels relative to M0 cells. Mean ± SE for n=3.

KEY RESEARCH ACCOMPLISHMENTS

- Optimization of methods for efficacious RNA isolation from laser microdissectates of formalin-fixed, paraffin-embedded non-small cell lung cancer specimens for global microarray-based microRNA profiling
- Global microRNA profiling of cancerous epithelial and non-cancerous stromal components of pathologic stage I non-small cell lung cancer
- Identification of significant biological effects in lung cancer cells of epithelial component-associated prognostic microRNA miR-372
- Identification of lung cancer prognosis-associated CA12 gene as a target of miR-372.
- Observation that the expression level of miR-146b likely does not affect M1/M2 polarization of macrophages.

REPORTABLE OUTCOMES

- A workflow for microRNA profiling of tumor epithelial and stromal components using formalin-fixed cancer tissues has been developed
- Epithelial and stromal component-specific microRNA profiles of NSCLC have been obtained for the first time.
- miR-372 overexpression makes lung cancer cells acquire a more “invasive” phenotype, in keeping with microRNA profiling experiments. Targeting of CA12 by miR-372 may underlie this phenomenon.
- miR-146b expression likely does not affect M1/M2 polarization of macrophages.

CONCLUSIONS

The biomarker signal that is associated with the prognostic values of tumor microRNA expression levels can arise from the cancerous epithelial component of tumors, as normally expected, as well as from the non-cancerous stromal component of the tumors, indicating a significant biological role of the tumor stroma (microenvironment) on the biology of non-small cell lung cancer. The findings of this project suggest that (1) the epithelial and stromal components of tumors are significantly different in terms of microRNA expression; (2) fold-change microRNA expression differences between stage I NSCLC tumors that later recur or do not recur obtained by tumor component-specific microRNA profiling are in the same range as that of whole tumor microRNA profiling; (3) ISH is probably not a good technique for the development of robust prognostic biomarkers for NSCLC; (4) miR-372 overexpression makes lung cancer cells more malignant, and targeting of CA12 by miR-372 may be one of the mechanisms that underlie this; and, (5) miR-146b expression likely does not affect M1/M2 polarization of macrophages.

REFERENCES

1. Goldstraw P, Crowley J, Chansky K, et al: The IASLC Lung Cancer Staging Project: proposals for the revision of the TNM stage groupings in the forthcoming (seventh) edition of the TNM Classification of malignant tumours. J Thorac Oncol 2:706-14, 2007
2. Patnaik SK, Kannisto E, Knudsen S, et al: Evaluation of microRNA expression profiles that may predict recurrence of localized stage I non-small cell lung cancer after surgical resection. Cancer Res 70:36-45, 2010
3. Nielsen BS, Jorgensen S, Fog JU, et al: High levels of microRNA-21 in the stroma of colorectal cancers predict short disease-free survival in stage II colon cancer patients. Clin Exp Metastasis 28:27-38, 2011
4. Hanna JA, Wimberly H, Kumar S, et al: Quantitative analysis of microRNAs in tissue microarrays by in situ hybridization. Biotechniques 52:235-45, 2012
5. Wang J, Tian X, Han R, et al: Downregulation of miR-486-5p contributes to tumor progression and metastasis by targeting protumorigenic ARHGAP5 in lung cancer. Oncogene 33:1181-9, 2014
6. Dweep H, Sticht C, Pandey P, et al: miRWalk--database: prediction of possible miRNA binding sites by "walking" the genes of three genomes. Journal of biomedical informatics 44:839-47, 2011
7. Voorhoeve PM, le Sage C, Schrier M, et al: A genetic screen implicates miRNA-372 and miRNA-373 as oncogenes in testicular germ cell tumors. Cell 124:1169-81, 2006
8. Ilie M, Hofman V, Zangari J, et al: Response of CAIX and CAXII to in vitro re-oxygenation and clinical significance of the combined expression in NSCLC patients. Lung cancer 82:16-23, 2013

9. Ilie MI, Hofman V, Ortholan C, et al: Overexpression of carbonic anhydrase XII in tissues from resectable non-small cell lung cancers is a biomarker of good prognosis. International journal of cancer. Journal international du cancer 128:1614-23, 2011

10. Raponi M, Dossey L, Jatkoe T, et al: MicroRNA classifiers for predicting prognosis of squamous cell lung cancer. Cancer Res 69:5776-83, 2009

11. Patnaik SK, Kannisto E, Mallick R, et al: Overexpression of the lung cancer-prognostic miR-146b microRNAs has a minimal and negative effect on the malignant phenotype of A549 lung cancer cells. PLoS One 6:e22379, 2011

12. Landgraf P, Rusu M, Sheridan R, et al: A mammalian microRNA expression atlas based on small RNA library sequencing. Cell 129:1401-14, 2007

13. Sica A, Mantovani A: Macrophage plasticity and polarization: in vivo veritas. J Clin Invest 122:787-95, 2012